

Confinement of test particles in warped spacetimes

Suman Ghosh* and Sayan Kar†

Department of Physics and Meteorology and Centre for Theoretical Studies

Indian Institute of Technology, Kharagpur 721 302, India

Hemwati Nandan‡

Centre for Theoretical Studies

Indian Institute of Technology,

Kharagpur 721 302, India

Abstract

We investigate test particle trajectories in warped spacetimes with a thick brane warp factor, a cosmological on-brane line element and a time dependent extra dimension. The geodesic equations are reduced to a first order autonomous dynamical system. Using analytical methods, we arrive at some useful general conclusions regarding possible trajectories. Oscillatory motion, suggesting confinement about the location of the thick brane, arises for a growing warp factor. On the other hand, we find runaway trajectories (exponential-like) for a decaying warp factor. Variations of the extra dimensional scale factor yield certain quantitative differences. Results obtained from explicit numerical evaluations match well with the qualitative conclusions obtained from the dynamical systems analysis.

Keywords: Geodesics, extra dimension, braneworld.

PACS numbers: 04.50.+h, 12.10.-g

* Electronic address: suman@cts.iitkgp.ernet.in

† Electronic address: sayan@cts.iitkgp.ernet.in

‡ Electronic address: hnandan@cts.iitkgp.ernet.in

I. INTRODUCTION

Much of the initial interest and subsequent research on the hypothesis that we live on an embedded, timelike submanifold (the brane) of a higher dimensional ($D > 4$) Lorentzian spacetime (warped or unwarped) was focused on the assumption that the scale of the extra dimension is independent of the coordinates. The original work of Randall and Sundrum (RS) [1, 2] on warped braneworlds, published a decade ago, did refer to the idea of the scale of the extra dimension being spacetime dependent, while addressing the issue of stability, in a two-brane scenario. In such a model, it is necessary to stabilise the inter-brane distance (modulus) to a fixed value, in order to avoid a collapse of one brane onto another. A spacetime dependent bulk scalar field, was used to achieve the desired stability of the two-brane system, through the Goldberger–Wise mechanism [3]. A good deal has since then been done with the assumption of a spacetime dependent radion field, including its effects, through various types of couplings, on particle phenomenology [4, 5] associated with the two-brane RS model.

In a single brane scenario or from a purely higher dimensional bulk perspective, the space-time dependence of the metric function(s) associated with the extra dimensional coordinate(s) basically imply that the scale of the extra dimension depends on the on-brane or four dimensional spacetime coordinates. To visualise this, it is easiest to go back to the standard Kaluza–Klein (KK) universe models with different scale factors associated with the evolution of each set of non-compact/compact dimensions (usual or extra). The difference between today’s warped braneworlds is the warped geometry and also the non-compact extra dimension(s). We shall be concerned with single brane scenarios in this article.

Since the early days of General Relativity, one possible way of understanding the nature of the gravitational field has been to study geodesics and geodesic deviation [6]–[8] in the given background geometry. While the spacetime variation of the connection reflects on the trajectories, the effects of curvature variations clearly control geodesic deviation. This is true in any dimension and in any metric theory of gravity. Usually, generic statements (eg. existence of orbits of different types, oscillatory/exponential behaviour in trajectories, focusing and defocusing etc.) and their relation to variations in the metric functions, are difficult to extract, though the primary goal in such studies (on geodesics) must always be so.

Over the years, several authors [9, 10, 11] have investigated the behaviour of geodesics in background geometries of various higher dimensional theories of gravity. Recently, in [12], it was shown briefly, that in warped product spacetimes it is possible to have classical confinement of test particles. In our work here, we confirm and add to the results in [12], through detailed analysis, both numerical and analytical.

Let us assume a bulk line element of the form,

$$ds^2 = e^{2f(\sigma)} [-dt^2 + a^2(t) d\mathbf{X}^2] + b^2(t) d\sigma^2, \quad (1.1)$$

where $d\mathbf{X}^2 = dx^2 + dy^2 + dz^2$. Here, the function $b(t)$ represents the scale of the extra dimension while the $a(t)$ and $e^{2f(\sigma)}$ are the usual cosmological scale and warp factors respectively. In what follows, we shall largely be concerned with the effect of the geometric properties of the bulk spacetime on the trajectories that can exist in them. We intend to delineate how features change when we vary the nature of each of the three functions $a(t)$, $b(t)$ and $f(\sigma)$. The geodesic equations cannot be solved analytically (modulo a few simplistic cases) in a spacetime as complicated as represented by (1.1). Thus, we make use of the dynamical systems approach as well as numerical methods, through which we are able to extract some useful information regarding the behaviour of trajectories. For numerical computations of the differential equations involved in this work, we have used standard numerical codes, with appropriate initial conditions on the variables associated with null and timelike geodesic evolution.

The paper is organised as follows. In the next Section, we elaborate on the spacetime geometry and discuss our choices for the functions $a(t)$, $b(t)$ and $f(\sigma)$ which we use henceforth. Then, in the subsequent Sections, we discuss the nature of geodesics in detail for our specific choices of the functions. Finally, we make a comparison of our results with those in certain limiting scenarios and conclude with a summary of the results obtained.

II. THE BACKGROUND SPACETIME GEOMETRIES

We consider the metric given by equation (1.1) rewritten in conformal time (η), as follows,

$$ds^2 = e^{2f(\sigma)} a^2(\eta) [-d\eta^2 + d\mathbf{X}^2] + b^2(\eta) d\sigma^2. \quad (2.1)$$

To arrive at concrete results in the following Sections, we need to choose the functional forms of the warp factor, cosmological and extra dimensional scale factors. For the warp

factor e^{2f} we choose,

$$f(\sigma) = \begin{cases} -\log(\cosh k\sigma) & \rightarrow \text{represents a decaying warp factor,} \\ \log(\cosh k\sigma) & \rightarrow \text{represents a growing warp factor,} \end{cases} \quad (2.2)$$

which correspond to the well-known thick brane models [13, 14]. In such models, the brane is dynamically generated as a scalar field domain wall (soliton) in the bulk. Note the warp factor in such models is a smooth function of the extra dimension, unlike the RS case where we have $f(\sigma) = -k|\sigma|$ (i.e. a function with a derivative jump—such branes are called thin branes). We choose to work with thick branes mainly to avoid the jumps and delta functions which will appear in the connection and curvature for thin branes.

What do we choose for the scale factors? Two different combinations of $a(\eta)$ and $b(\eta)$, chosen as models to represent different kinds of time evolution, are given below in terms of the cosmological time “ t ”,

$$\{a(t), b(t)\} = (i) \{a_0 t^{\nu_1}, b_0 + b_1 t^{-\nu_2}\}, \quad \text{and} \quad (ii) \{a'_0 e^{H(t-t_0)}, b'_0 + b'_1 e^{-\beta H(t-t_0)}\}, \quad (2.3)$$

where we take ν_1 to span over an open interval $(0, 1)$, so that in (i) $a(t)$ represents an expanding but decelerating on-brane line element (which is radiative for $\nu_1 = \frac{1}{2}$), and in (ii) we take H to be positive, representing an accelerating de-Sitter on-brane line element. $b_0, b_1, \nu_2, b'_0, b'_1$ and β are positive so that we have a decaying extra dimension which stabilizes to a finite value as $t \rightarrow \infty$. The type of metric functions we consider here may be obtained as analytic solutions of the five dimensional Einstein equations with the corresponding Einstein tensors providing matter energy-momentum profiles through the Einstein field equations. As shown in [15], for similar metric functions, the corresponding matter stress-energy can indeed satisfy the Weak Energy Condition.

In the first case, the conformal time $\eta = \int \frac{dt}{a_0 t^{\nu_1}}$. We choose to work with an initial condition such that at $t = t_0$, $\eta = \eta_0 = 1$ which, in turn, implies $a_0 = \frac{t_0^{1-\nu_1}}{1-\nu_1}$ and $\eta = \left(\frac{t}{t_0}\right)^{1-\nu_1}$ where the domain of η is $1 < \eta < \infty$. We also assume that evolution of our universe begins at $t = t_0$ (or $\eta = 1$) when the scales of ordinary and extra space dimensions were same (i.e. $a(t_0/\eta_0) = b(t_0/\eta_0)$). In terms of conformal time, we are led to,

$$a(\eta) = \frac{t_0}{1-\nu_1} \eta^{\frac{\nu_1}{1-\nu_1}} \quad \text{and} \quad b(\eta) = \frac{t_0}{1-\nu_1} - \frac{b_1}{t_0^{\nu_2}} \left(1 - \eta^{\frac{-\nu_2}{1-\nu_1}}\right). \quad (2.4)$$

The stabilization condition further implies,

$$b_0 = \frac{t_0}{1-\nu_1} - \frac{b_1}{t_0^{\nu_2}} > 0 \quad \text{or} \quad b_1 < \frac{t_0^{1+\nu_2}}{1-\nu_1}. \quad (2.5)$$

In order to reduce the number of free parameters, we consider $b_1 = t_0^{1+\nu_2}$ (which is, in fact, the maximum possible value for b_1) as ν_1 can only be close to zero (but not equal to zero). Therefore we have,

$$b(\eta) = t_0 \left(\frac{\nu_1}{1-\nu_1} + \eta^{\frac{-\nu_2}{1-\nu_1}} \right). \quad (2.6)$$

Using a similar prescription for the de-Sitter model, we obtain,

$$a(\eta) = \frac{1}{H} \frac{1}{(1-\eta)} \quad \text{and} \quad b(\eta) = \frac{1}{H} \left[1 - b'_1 H \{ 1 - (1-\eta)^\beta \} \right], \quad (2.7)$$

where $b'_1 H < 1$ and $0 < \eta < 1$. Let us consider, $\nu_1 = \nu_2 = \frac{1}{2}$, $t_0 = 1$, $H = 1$, $b'_1 = \frac{1}{2}$ and $\beta = 1$ which leads to the following two different combinations of the scale factors,

$$\begin{aligned} \text{(A)} \quad & a(\eta) = 2\eta, \quad b(\eta) = 1 + \frac{1}{\eta}, \\ \text{(B)} \quad & a(\eta) = \frac{1}{1-\eta}, \quad b(\eta) = 1 - \frac{\eta}{2}. \end{aligned}$$

These combinations of scale factors will henceforth be abbreviated as set (A) and set (B). Fig. 1 gives a pictorial representation of the warp factors (decaying and growing) and the scale factors corresponding to set (A) and set (B).

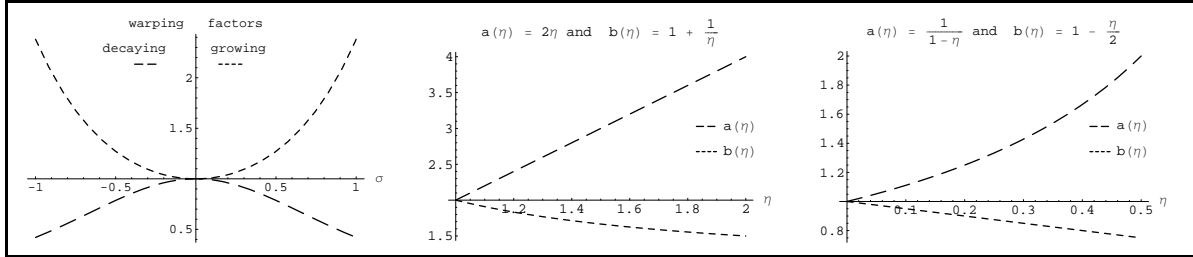


FIG. 1: Variations of warp factors and the scale factors for set(A) and set(B) respectively.

III. GEODESICS

The general form of the constraint (i.e. $g_{AB}u^A u^B = -\epsilon$) for null and timelike geodesics corresponding to the metric (2.1) is given below,

$$e^{2f(\sigma)} a^2(\eta) [-\dot{\eta}^2 + \dot{\mathbf{X}}^2] + b(\eta)^2 \dot{\sigma}^2 + \epsilon = 0, \quad (3.1)$$

where $\epsilon = 1$ and 0 denote the cases corresponding to the timelike and null geodesics respectively and a dot here represents the differentiation with respect to the affine parameter λ .

As x_i (such that $x_1 = x$, $x_2 = y$, and $x_3 = z$) is cyclic, an obvious conclusion for the metric (2.1) is,

$$\dot{x}_i = \frac{D_i e^{-2f}}{a^2}, \quad (3.2)$$

where D_i 's are integration constants. The effective geodesic potentials V_σ and V_x are then calculated as,

$$V_\sigma(\lambda) = \frac{\epsilon + a^2(\eta) e^{2f(\sigma)} (-\dot{\eta}^2 + 3\dot{x}^2)}{2b^2}, \quad (3.3)$$

$$V_x(\lambda) = \frac{1}{6} \left[\dot{\eta}^2 + \frac{\epsilon + b^2 \dot{\sigma}^2}{e^{2f(\sigma)} a^2(\eta)} \right] = -\frac{D_i^2 e^{-4f(\sigma)}}{2a^4(\eta)}, \quad (3.4)$$

where we have considered $\dot{x} = \dot{y} = \dot{z}$, which will be used throughout hereafter. In order to find $V_\sigma(\sigma)$ (or $V_x(x)$), we shall make use of solutions for $x(\lambda)$, $\eta(\lambda)$ and $\sigma(\lambda)$ in the right hand side of equation (3.3) (or equation (3.4)) and, subsequently, make a parametric plot of $V_\sigma(\lambda)$ versus $\sigma(\lambda)$ (or $V_x(\lambda)$ versus $x(\lambda)$) to arrive at a pictorial representation of $V_\sigma(\sigma)$ (or $V_x(x)$). It may be noted that, we have absorbed the factor “ ϵ ” in the effective geodesic potential. Therefore, for both timelike and null geodesics, we are essentially looking at test particles with zero “total energy” (from a mechanics point of view).

A. Dynamical systems analysis

The geodesic equations corresponding to the metric (2.1) derived for general warp and scale factors turn out to be,

$$\ddot{\eta} + \frac{a'(\eta)}{a(\eta)} [\dot{\eta}^2 + \sum_i (\dot{x}_i)^2] + e^{-2f(\sigma)} \frac{b(\eta)b'(\eta)}{a^2(\eta)} \dot{\sigma}^2 + 2f'(\sigma) \dot{\eta} \dot{\sigma} = 0, \quad (3.5)$$

$$\ddot{x}_i + \frac{2a'(\eta)}{a(\eta)} \dot{\eta} \dot{x}_i + 2f'(\sigma) \dot{x}_i \dot{\sigma} = 0, \quad (3.6)$$

$$\ddot{\sigma} + \frac{2b'(\eta)}{b(\eta)} \dot{\eta} \dot{\sigma} - f'(\sigma) e^{2f(\sigma)} \frac{a^2(\eta)}{b^2(\eta)} [-\dot{\eta}^2 + \sum_i (\dot{x}_i)^2] = 0, \quad (3.7)$$

here the dots represent the differentiation with respect to the affine parameter λ (or an arbitrary parameter, for null geodesics) while primes denote differentiation of the functions with respect to their corresponding independent variables, η or σ . The geodesic equations corresponding to x , y , and z can be reproduced from equation (3.6) and they all have an identical structure except for the constants D_i . The full geodesic equations in a spacetime corresponding to the metric (2.1) are very difficult to solve analytically. However, the Eqs

(3.5)-(3.7) can be recast as the following dynamical system of first order, coupled differential equations,

$$\dot{\eta} = \frac{e^{-f(\sigma)}}{a(\eta)} \sqrt{\epsilon + \frac{\chi^2}{b^2(\eta)}}, \quad (3.8)$$

$$\dot{x}_i = \frac{D_i e^{-2f(\sigma)}}{a^2(\eta)}, \quad (3.9)$$

$$\dot{\sigma} = \frac{\chi}{b^2(\eta)}, \quad (3.10)$$

$$\text{and } \dot{\chi} = -f'(\sigma) \left(\epsilon + \frac{\chi^2}{b^2(\eta)} \right). \quad (3.11)$$

It will be interesting to see if one can analytically draw some useful conclusions about the behaviour of the geodesics by using the above set of equations. For the growing warp factor, $f'(\sigma) \sim \tanh(k\sigma)$ and if we expand this function about the location of the brane (i.e. $\sigma = 0$), the dominant term in the neighbourhood of that point will be linear in σ . In such a scenario, for the timelike case ($\epsilon = 1$), the Eqs (3.10) and (3.11) resemble the following equations,

$$\dot{\sigma} \sim \chi \times \text{positive terms}, \quad \text{and} \quad \dot{\chi} \sim -\sigma \times \text{positive terms}, \quad (3.12)$$

which are qualitatively similar to a dynamical system representing simple harmonic motion (SHM) $\{\dot{X} = P, \dot{P} = -X\}$ (modulo a multiplicative factor). From this consideration, one can intuitively argue that the Eqs (3.8)-(3.11) will have oscillatory solutions for σ and χ (though, not *simple* harmonic). On the other hand, for a decaying warp factor, $f(\sigma) = -\log(\cosh k\sigma)$, the above set of equations given by (3.12) lead to a system with exponential solutions. Thus, there should not be any oscillatory trajectories with decaying warp factors.

From equation (3.12), it is also evident that, for *any* growing warp factor one does not have oscillatory timelike trajectories. For example, in the Randall–Sundrum scenario, we have, $f(\sigma) \sim |\sigma|$ and $f'(\sigma)$ is therefore a step function, which cannot have an expansion with a term linear in σ . So there exist no oscillatory solution for this case.

In order to further analyse the behavior of trajectories analytically, let us look at the specific case where $b(\eta)$ is a constant (say $b(\eta) = 1$). Since we are particularly interested about motion in the bulk, we choose, $\dot{x}_i = 0$ (as x_i does not appear in the other three equations i.e. in (3.8), (3.10), and (3.11)). With these considerations, we arrive at following

set of equations,

$$\dot{\eta} = \frac{e^{-f(\sigma)}}{a(\eta)} \sqrt{\epsilon + \chi^2}, \quad (3.13)$$

$$\dot{\sigma} = \chi, \quad (3.14)$$

$$\text{and } \dot{\chi} = -f'(\sigma) (\epsilon + \chi^2). \quad (3.15)$$

For timelike geodesics and growing warp factors, from Eqs (3.14) and (3.15), we obtain,

$$\frac{d\sigma}{d\chi} = -\frac{\chi}{(1 + \chi^2) \tanh \sigma} \implies C_1 \operatorname{sech} \sigma = \sqrt{1 + \chi^2}, \quad (3.16)$$

where C_1 is an integration constant. Similarly, Eqs (3.13), (3.15) and (3.16) further lead to,

$$\frac{d\chi}{d\eta} = -2\eta \sqrt{C_1^2 - 1 - \chi^2} \implies \chi = \sqrt{C_1^2 - 1} \sin(C_2 - \eta^2), \quad (3.17)$$

where C_2 is another integration constant. Now combining the Eqs (3.16) and (3.17), one easily obtains,

$$\sigma = \operatorname{sech}^{-1} \left[\frac{1}{C_1} \sqrt{1 + (C_1^2 - 1) \sin^2 (C_2 - \eta^2)} \right]. \quad (3.18)$$

The argument of the “ sech^{-1} ” function contains a sinusoidal part which guarantees an oscillatory behaviour of $\sigma(\eta)$, though its details depend on the parameters (C_1 and C_2) involved in the analysis. It is worth mentioning here that even if we let $a(\eta)$ to be a constant, oscillations persist (only the factor $\sin^2(C_2 - \eta^2)$ gets replaced by $\sin^2(C_2 - 2\eta)$). This confirms that the oscillations are solely due to the presence of a growing warp factor. It has been checked that, for a decaying warp factor, no such analytic expression can be found. In fact, the Eqs (3.8), (3.10) and (3.11) form a dynamical system of their own, irrespective of equation (3.9). Unfortunately, with $\epsilon = 1$, this system does not have any fixed points for a finite value of η . But, for a static extra dimension, we can investigate the solution space [16] for the following set of two equations,

$$\dot{\sigma} = \chi, \quad \text{and} \quad \dot{\chi} = \pm(1 + \chi^2) \tanh k\sigma, \quad (3.19)$$

where $+$ and $-$ signatures denote the decaying and growing warp factors respectively. It can easily be shown that the point $(\sigma, \chi) = (0, 0)$ is a saddle point in the phase space for the decaying warp factor and a centre in case of a growing warp factor. Thus, we can expect oscillatory solutions for $\sigma(\lambda)$ and $\chi(\lambda)$ in the latter case (i.e. for a growing warp factor). We present the phase space plots of σ and χ with two different warp factors in

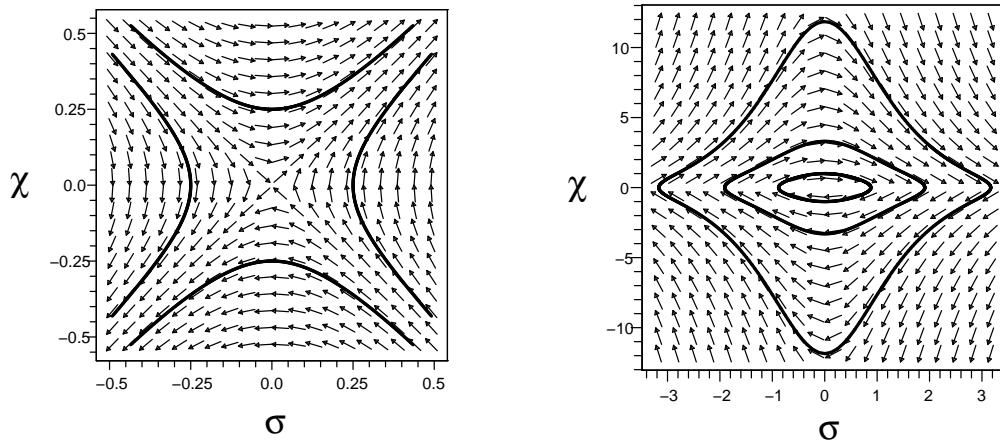


FIG. 2: The solid lines indicate different flows in the solution space of $\{\sigma, \chi\}$ for different initial conditions, such as, in the left plot (for decaying warp factor): $\{\sigma(0), \chi(0)\} = (0.25, 0), (0, -0.25), (-0.25, 0), (0, 0.25)$ (here λ runs from -1.3 to 1.3), and in the right plot (for growing warp factor): $\{\sigma(0), \chi(0)\} = (0, 1), (1, 2), (2, 3)$ (here λ runs from 0 to 6.5).

the Fig. 2. A decaying warp factor only helps a particle to move away from the brane, except for the initial conditions satisfying $\sigma + \chi = 0$ (where the particle tends toward the location of the brane with an ever-decreasing velocity). This essentially means that only for the abovementioned initial conditions, particles will end up accumulating near the brane with increasing affine parameter. Particles with initial condition $\sigma - \chi = 0$ will be repelled away from the brane. There are two other kinds of trajectories. The trajectories in the quadrants $(\sigma + \chi > 0, \sigma - \chi < 0)$ and $(\sigma + \chi < 0, \sigma - \chi > 0)$ may cross the brane at some point of time (depending on the initial conditions), and the trajectories in the quadrants $(\sigma + \chi > 0, \sigma - \chi > 0)$ and $(\sigma + \chi < 0, \sigma - \chi < 0)$ will bypass the location of the brane (though they may come very close, depending on the initial conditions). On the other hand, the closed curves, in the case with a growing warp factor, indicate that, $\sigma(\lambda)$ and $\chi(\lambda)$ have an oscillatory behaviour. One can also notice that the nature of the oscillations depend heavily on the initial conditions. A particle, initially on or close to the brane and having a small velocity, executes an almost sinusoidal oscillation. This oscillatory pattern will tend towards a square wave profile as the distance of the launching point from the brane, or the initial velocity, increases. The phase portraits in Fig. 2 are for a static extra dimension. We expect to see a similar solution space for a dynamic extra dimension ($b(\eta)$) too when

$\eta \rightarrow \infty$ because according to our choices $b(\eta)$ gets stabilised to a constant value for large η . The closed trajectories for a static extra dimension and a growing warp factor would become limit cycles in phase space when we have a dynamic extra dimension.

One may also note that for null geodesics, the eigenvalues of the linearised system at the origin in the phase space vanishes. It is therefore not possible to comment on the solution space for this case.

B. Numerical evaluations

The full geodesic Eqs (3.5)-(3.7) for the null and timelike geodesics can obviously be solved numerically. We present some features of these geodesics, graphically, with the set (A) and (B) for the scale factors and with the growing and decaying warp factors of the thick brane model. All of these cases are presented in Figs. 3 -8 where the figure captions are self-explanatory and describe the corresponding results. We have shown the solutions for timelike and null geodesics in the case with a growing warp factor. Here, we have observed remarkable differences between the null and timelike cases (see Figs. 4, 5, 7 and 8). Otherwise, where the differences between the results for timelike and null cases are small (i.e. results remain qualitatively similar for the case of a decaying warp factor), we present only the timelike geodesics (see Figs. 3 and 6). The initial conditions for our numerical evaluations are chosen as $\dot{x} = \dot{y} = \dot{z} = \dot{\sigma} = 0.1$ at $\lambda = 0$ and $\dot{\eta}$ at $\lambda = 0$ is calculated by using the null and timelike constraints which differs between models.

We have observed that for a growing warp factor, the timelike geodesics have an oscillatory behaviour for both the cases (i.e. set (A) and (B)) as presented in Figs. 4 and 7 respectively. Such an oscillatory behaviour is absent in the trajectories of null geodesics in all the cases. This essentially means that massless particles are free to escape into the bulk. The oscillatory behaviour of the timelike geodesics for a growing warp factor also manifests itself in terms of the potential $V(\sigma)$ as shown in Figs. 4 and 7 for set (A) and set (B) respectively. The fact which is worth mentioning about these trajectories is that a massive particle never moves away to an infinite distance from the location of the brane. It seems that the trajectories are automatically localised on or near the brane in the presence of a growing warp factor. The potential in this case is in fact that of an anharmonic oscillator where both the amplitude and frequency of the oscillations are monotonically increasing and converging towards a limiting

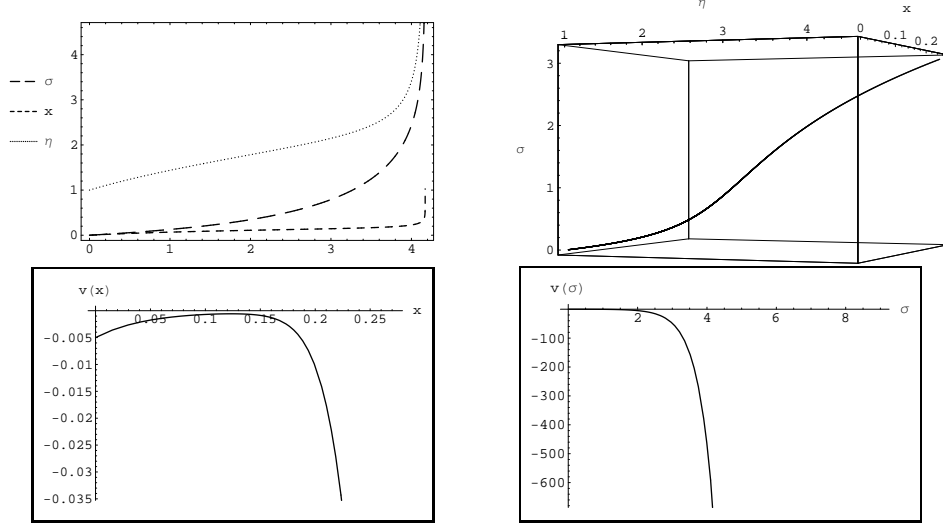


FIG. 3: Timelike geodesics for set (A) with a decaying warp factor.

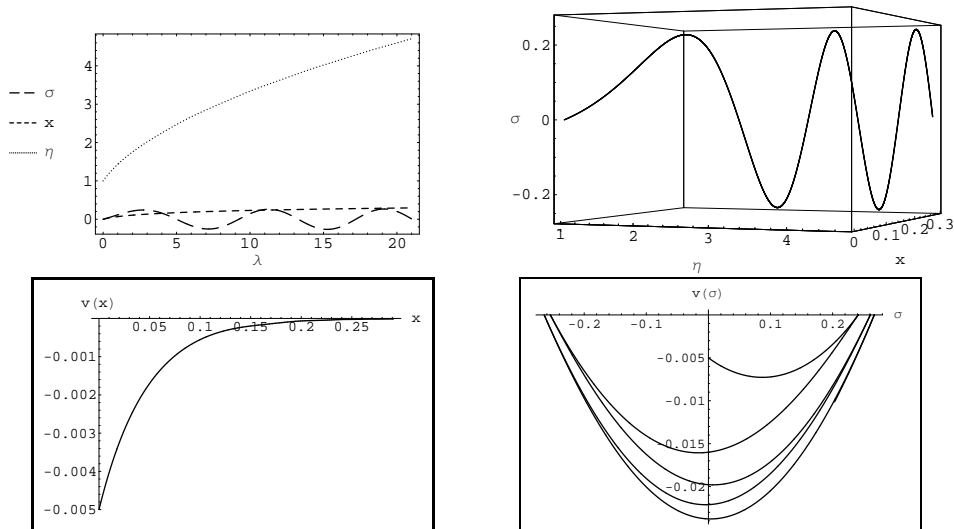


FIG. 4: Timelike geodesics for set (A) with a growing warp factor.

value with an increasing λ . We will again return to the interpretation of this feature in terms of the warp factor and the scale of the extra dimension, in the Section IV. Our numerical findings in this section tally well with the results found earlier in Section III, via the analysis of an autonomous dynamical system derived from geodesic equations.

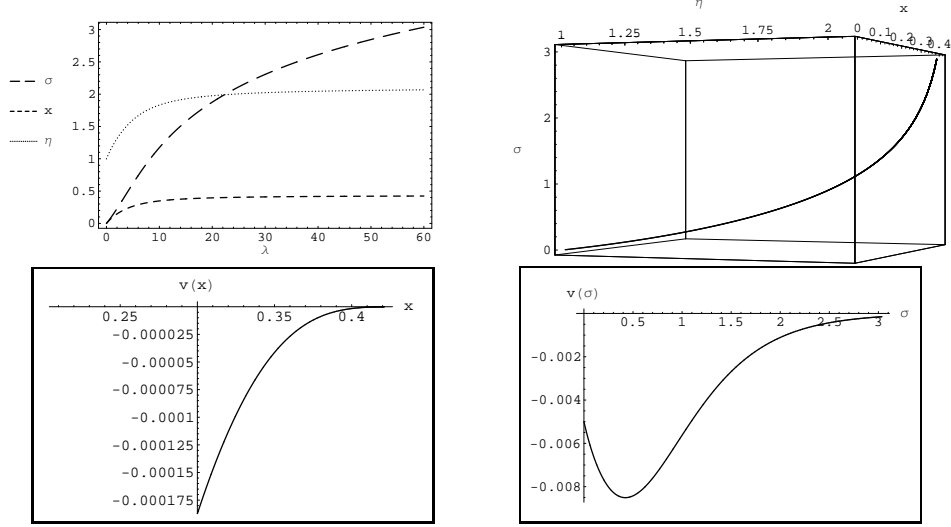


FIG. 5: Null geodesics for set (A) with a growing warp factor.

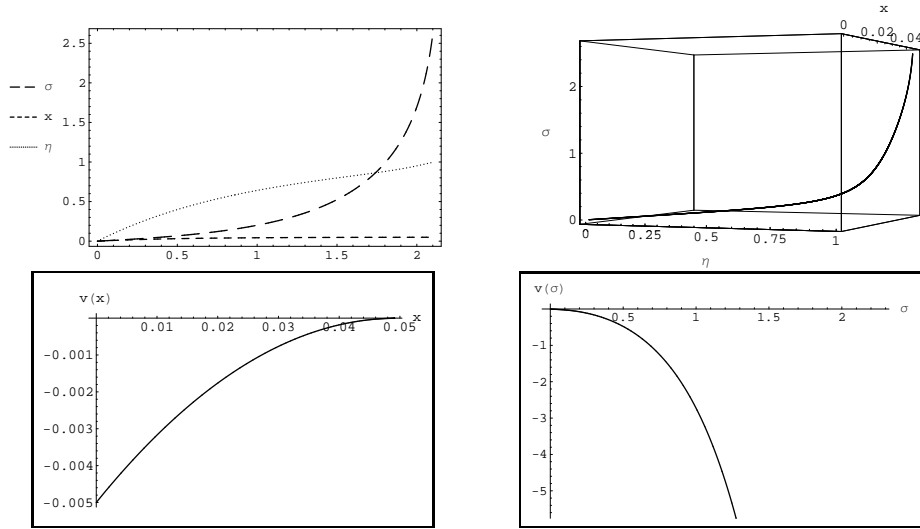


FIG. 6: Timelike geodesics for set (B) with a decaying warp factor.

IV. EFFECTS OF WARPING AND TIME DEPENDENCE IN EXTRA DIMENSION SCALE AND CONFINEMENT OF TEST PARTICLES

In order to figure out the effects of warping and a time dependent extra dimension, we will compare the generalised braneworld scenario (discussed in the previous section) with the situations where we do not have any warp factor or a time dependence in the extra dimension scale. Let us first consider, the metric (2.1) without the warping factor. This

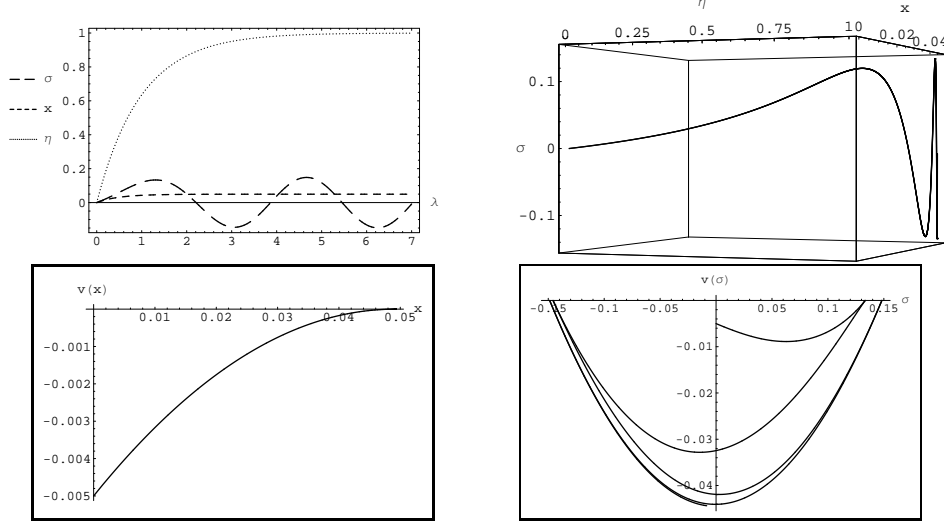


FIG. 7: Timelike geodesics for set (B) with a growing warp factor.

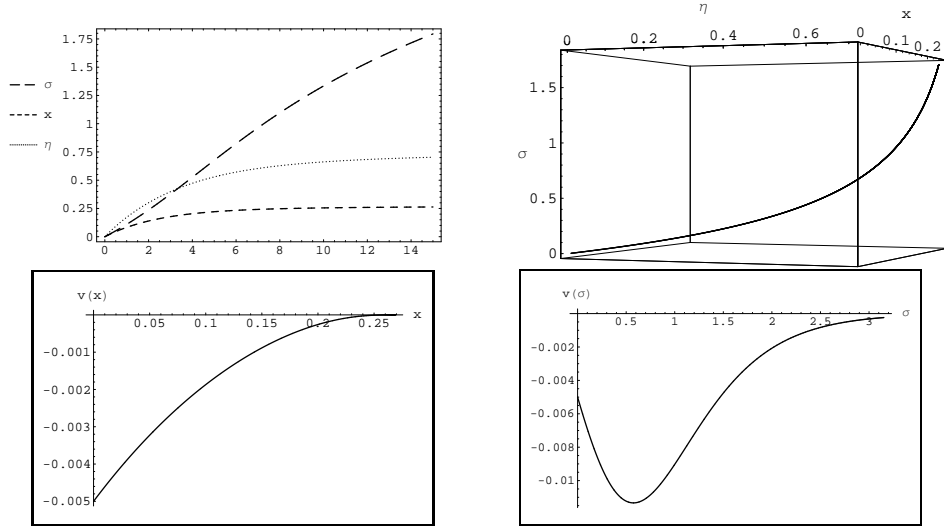


FIG. 8: Null geodesics for set (B) with a growing warp factor.

leads to the following constraint,

$$a^2(\eta) [-d\eta^2 + d\mathbf{X}^2] + b(\eta)^2 \dot{\sigma}^2 + \epsilon = 0. \quad (4.1)$$

Now σ becomes cyclic in the geodesic Lagrangian and gives us $V_x(x) = -D^2/(2a^4)$ and $V_\sigma(\sigma) = -P^2/(2b^4)$ which eventually lead to,

$$\lambda = \int \frac{a d\eta}{\sqrt{\left(\epsilon + \frac{D^2}{a^2} + \frac{P^2}{b^2}\right)}}. \quad (4.2)$$

With a nonzero P , we could not find an analytic solution for Eq. 4.2 (though it is exactly solvable for $P = 0$). We have therefore solved the geodesic equations for $P \neq 0$ numerically.

In the case where $b(\eta)$ is constant, the constraint (3.1) gives,

$$\frac{d\eta}{d\lambda} = \frac{e^{-f}}{a} \sqrt{\left(\epsilon + \dot{\sigma}^2 + \frac{D^2}{a^2 e^{2f}} \right)}. \quad (4.3)$$

The Eq. (4.3) is also not analytically solvable except for the case with $D = 0$. As above, we solve the geodesic equations numerically for the general situation when $D \neq 0$.

In order to see the specific differences between the general case (eg. timelike geodesics for set (A) with growing warp factor as shown in Fig. 4), and two of its subcases (one without a warping factor and the other with a static extra dimension), the plots of the potential $V_\sigma(\sigma)$ and the trajectories for both of these two subcases are presented in Fig. 9. Here, we have considered $D = 1$ and $P = 1$ for the purpose of numerical computations. The differences between the two subcases are quite clearly visible. We have also worked through other similar cases, which we do not mention here. It is clear that the oscillatory behaviour

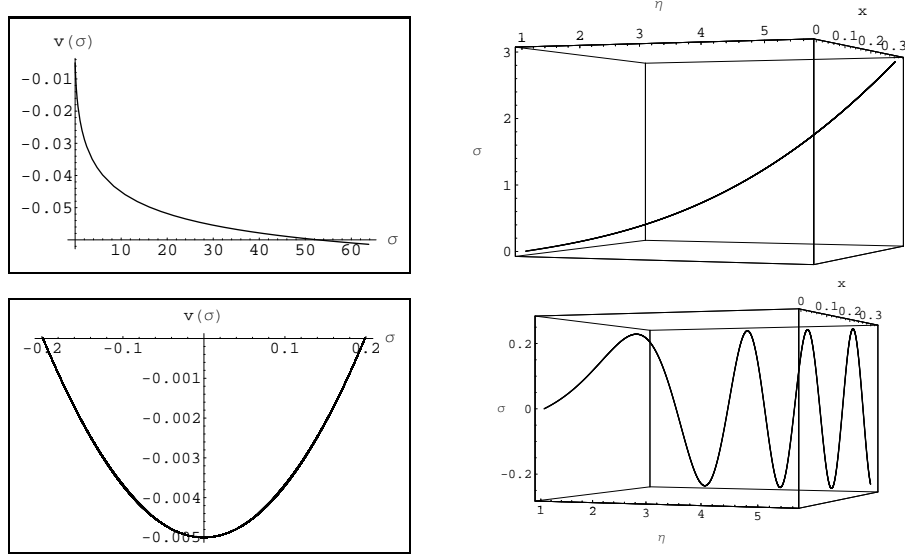


FIG. 9: Plots in the upper and lower rows show the timelike geodesics for set (A) (with $b(\eta) = \text{constant}$) for models without any warping factor and with growing warp factor respectively.

is due to the presence of a growing warp factor (as already argued in Section III). If we compare Fig. 9 with Fig. 4, where scale of the extra dimension is dynamic, the increase in the amplitude and frequency of the oscillations of σ , may be understood as an effect of the decay in the scale of the extra dimension $b(\eta)$. In fact, the scale $b(\eta)$, as mentioned before, can be viewed as the length of an anharmonic oscillator which tends to become a harmonic one with an increasing value of the affine parameter. In other words, this problem

is equivalent to a problem of a particle in a one dimensional box whose size is decreasing and tending to a finite value. This is exactly how one can understand the increase in the amplitude of the oscillation in $\sigma(\lambda)$, in Fig. 4, and its eventual stabilisation to a limiting value. Such features are also evident from the behaviour of the corresponding potentials as given in the Figs. 4 and 9.

Let us try to understand the above-mentioned confinement from a different point of view. It was shown in [12], that in the case of a five dimensional bulk with a static extra dimension and a growing warp factor (which is indeed a solution of five dimensional Einstein equations in presence of a negative bulk cosmological constant), we have confinement of test particles. Further, in [12], it was shown that confinement will be achieved if the following energy condition holds,

$$({}^0\hat{R}_{AB}e_\alpha^A e_\beta^B - {}^0R_{\alpha\beta})u^\alpha u^\beta > 0, \quad A, B = 0, 1, 2, 3, 4; \quad \alpha, \beta = 0, 1, 2, 3 \quad (4.4)$$

where, $e_\alpha^A = \frac{\partial x^A}{\partial y^\alpha}$ are the four basis vectors and $\{x^A\}$ and $\{y^\alpha\}$ are five and four dimensional coordinate systems respectively. \hat{R}_{AB} and $R_{\alpha\beta}$ are Ricci tensors in the bulk and on the $\sigma = \text{const.}$ hypersurface respectively. The above condition implies that the local gravitational density of five dimensional bulk matter, as measured by an observer freely falling along a hypersurface $\sigma = 0$ (or the brane), has to be greater than the gravitational density of the effective four dimensional matter. For the five dimensional geometry given by Eq. 2.1, the above constraint leads to

$$\frac{f'' + 4f'^2}{a^2 b^2} + \left(\frac{\dot{a}\dot{b}}{ab} - \frac{\ddot{b}}{b} \right) u^{02} + \frac{\dot{a}\dot{b}}{ab} \sum_{i=1}^3 u^{i2} > 0. \quad (4.5)$$

It may be noted that for a static extra dimension, i.e. when $b(\eta) \sim \text{constant}$, the following condition,

$$f'' + 4f'^2 > 0 \quad (4.6)$$

is sufficient for confinement of test particles. This condition is clearly satisfied for the functional form of the growing warp factor we have considered.

Now the constraint Eq. 4.5 is always satisfied for a monotonically growing warp factor with a growing $a(\eta)$ and a growing but decelerating $b(\eta)$. In that case, if $b(\eta)$ does not stabilise, then as $\eta \rightarrow \infty$, the depth of the potential well tends to zero (as $b(\eta)$ appears in the denominator of Eq. 3.3). As a result, confined trajectories will become more and

more unstable against perturbations and particles should disappear from the brane. This observation should rule out the models with growing and divergent $b(\eta)$, for example, some of the power law solutions (for $b(t)$) found in [15], in presence of different bulk matter fields as such. On the other hand, if $b(\eta)$ grows but stabilises to a finite value as $\eta \rightarrow \infty$, trajectories are confined, though become less strongly bound as the depth of the potential decreases (towards a limiting value).

The last two terms in the left hand side of 4.5 are always negative for a growing $a(\eta)$ and a decaying $b(\eta)$. Therefore, it is obvious that the inequality 4.5 will not always hold for any set of metric functions (though it happens to be the case for the metric functions we choose). However, one can argue that as $b(\eta)$ stabilises with $\eta \rightarrow \infty$, constraint 4.5 converges toward constraint 4.6. It is thus implied that confinement will eventually be achieved during the course of cosmological evolution. The trajectories, in this case, will also be more strongly bound as the depth of the potential well increases. It is worth mentioning here that, if $b(\eta)$ decays to a zero value, the depth the potential 3.3 tends to infinity resulting in an ever-growing amplitude of oscillation which eventually diverges. This aspect may help us rule out models with the $b(\eta)$ decaying to zero (instead of stabilising to a finite limiting value).

One may also find a constraint on the warp factor, for confinement, in a static bulk in the following simple way. For the test particles (moving along the extra dimension) to be confined somewhere in the bulk, their geodesic potential should have a minimum at that point. Now the corresponding geodesic potential is given by

$$V(\sigma) = -\frac{Ce^{-2f(\sigma)} - \epsilon}{2}, \quad (4.7)$$

where C is, a positive constant, dependent on the initial conditions. $V(\sigma)$ should have a minima at $\sigma = \sigma_0$, where $f'(\sigma_0) = 0$ and $e^{-2f(\sigma_0)} \neq 0$, if the following condition holds

$$f''(\sigma_0) > 0, \quad (4.8)$$

which means the $f(\sigma)$ must be a monotonically growing function of σ about the location where the potential has a minimum. For $f(\sigma) = \log(\cosh \sigma)$, $V(\sigma) = -\frac{C \operatorname{sech}^2 \sigma - \epsilon}{2}$. The minimum value of this potential for timelike geodesics is $-\frac{C-1}{2}$ (where $C \geq 1$) at $\sigma = 0$ and it reaches its maximum value $+\frac{1}{2}$ as $\sigma \rightarrow \pm\infty$. Therefore the zero energy trajectories are bounded within the σ values which can be obtained by equating $V(\sigma) = 0$. This leads to

$$f(\sigma) = \log \sqrt{C}. \quad (4.9)$$

We can therefore explain the confinement of massive particles in the context of Figs 4 and 6. On the other hand, for null geodesics, the zero energy trajectories always have runaway features (Figs. 5 and 8).

We note that whenever Eq. 4.8 is true, the Eq. 4.6 is automatically satisfied. This also justifies why geodesics in a thick braneworld model with growing warp factor i.e. $f(\sigma) \sim \log(\cosh \sigma)$ are confined near $\sigma = 0$, whereas with a decaying warp factor we don't see such confinement.

V. SUMMARY AND CONCLUSIONS

To conclude, we provide below a summary of the results obtained, in a systematic way.

- We have studied geodesics for the warped background geometry of a thick braneworld model with a cosmological metric on the brane and a time dependent extra dimension, in detail. Our choices for the scale factors (marked as set (A) and set (B) throughout this article) illustrate situations corresponding to decelerating (i.e. set (A)) and accelerating (i.e. set (B)) universes. The extra dimensional scale is chosen appropriately which stabilises to a constant value at large time.
- The geodesic equations in such a background can be rewritten as a first order autonomous dynamical system. Analytical insights as well as some specific solutions can therefore be obtained. In particular, the analysis of these equations as a dynamical system shows the role of the warp factor (growing/decaying) in controlling the nature of the solutions (oscillatory/exponential).
- Apart from a few specific cases, the geodesic equations, in general, can only be solved numerically since they are highly coupled differential equations. However, we are able to demonstrate some qualitative features of the dynamical system through numerical investigations. Detailed features of the null and timelike geodesics are brought out for different cases with growing and decaying warp factors. It may be noted that a numerical estimation is always possible for any other combination of scale factors/warp factor.
- We have tried to separate out the individual effects of the warp factor and the extra dimensional scale factor. It is found that the emergence of an oscillatory behaviour

in timelike geodesics (absent in the case of null geodesics) is essentially due to the presence of a growing warp factor. It seems that massive particles are constrained to be confined near the brane in this particular scenario (growing warp factor), while massless particles like photons or gravitons can indeed access the bulk. This observation is important in the context of localisation of fields on the brane. The behaviour of localisation of test particles in a geometry with a growing warp factor is reminiscent of fermion localisation with a growing warp factor. Even in the presence of a decaying warp factor, particles can also be localised though very special initial conditions are required. The effect of a dynamical (time dependent) extra dimension on the trajectories is found to be largely quantitative.

- We have clearly demonstrated that the analysis of geodesic motion obtained through a dynamical systems analysis matches quite well with the numerical computations.
- We have briefly examined a confinement condition obtained in [12] for our cases here. We also provide our comments on aspects of this condition and show that the issue of confinement puts important constraints on possible dynamic behaviour of the extra dimension.

We mention that it would be useful to investigate geodesic deviation and the kinematics of geodesic flows in a bulk geometry with a thick brane. In the latter case, we need to solve the geodesic and Raychaudhuri equations simultaneously, in order to obtain the evolution and initial condition dependencies of the kinematical quantities: expansion, rotation and shear (or ESR). We believe that such work may improve our understanding about the nature of warped extra dimensions. We hope to report on related work on the above-mentioned aspects, at a later stage.

Acknowledgments

SG thanks Indian Institute of Technology (IIT), Kharagpur, India for financial support and Centre for Theoretical Studies, IIT Kharagpur, India for allowing him to use its research facilities. The authors (SK and HN) sincerely thank the Department of Science and Technology (DST), Government of India for financial support (grant number: SR/S2/HEP-10/2005).

We also thank P. S. Dutta for some useful discussions.

-
- [1] L. Randall and R. Sundrum, Phys. Rev. Lett. **83**, 3370 (1999).
 - [2] L. Randall and R. Sundrum, Phys. Rev. Lett. **83**, 4690 (1999).
 - [3] W. D. Goldberger and M. B. Wise, Phys. Rev. Lett. **83**, 4922 (1999).
 - [4] C. Csaki, J. Hubisz, and S. J. Lee, Phys. Rev. D **76**, 125015 (2007);
C. Csáki, M. Graesser, L. Randall and J. Terning, Phys. Rev. D **62**, 045015 (2000);
C. Csáki, M. L. Graesser and G. D. Kribs, Phys. Rev. D **63**, 065002 (2001);
 - [5] G. F. Giudice, R. Rattazzi and J. D. Wells, Nucl. Phys. B **595**, 250 (2001);
T. Tanaka and X. Montes, Nucl. Phys. B **582**, 259 (2000);
D. Dominici, B. Grzadkowski, J. F. Gunion and M. Toharia, Nucl. Phys. B **671**, 243 (2003);
J. F. Gunion, M. Toharia and J. D. Wells, Phys. Lett. B **585**, 295 (2004).
 - [6] R. M. Wald, *General Relativity*, (University Chicago Press, Chicago, 1984).
 - [7] P. S. Joshi, *Global aspects in gravitation and cosmology*, (Oxford University Press, Oxford, UK, 1997).
 - [8] J. B. Hartle, *Gravity: An Introduction to Einstein's General Relativity*, (Pearson Education Inc., Singapore, 2003).
 - [9] J. Ponce de Leon, Int. J. Mod. Phys. D **12**, 757 (2003);
W. Mueck, K. S. Viswanathan and I. V. Volovich, Phys. Rev. D **62**, 105019, (2000);
D. Youm, Mod. Phys. Lett. A **16**, 2371 (2001);
F. Dahia, C. Romero, L. F. P. Silva and R. Tavakol, J. Math. Phys. **48**, 072501 (2007);
S. Guha and S. Chakraborty, **arXiv: 0812.5072**;
S. Das, S. Ghosh, J-W. van Holten and S. Pal, **arXiv:0902.2304**.
 - [10] S. Pal, *Gravitational Aspects of Warped Braneworld Models*, Ph.D. Thesis (2006), Jadavpur University, Kolkata, India and references therein.
 - [11] R. Koley, S. Pal and S. Kar, Am. J. Phys. **71**, 1037 (2003).
 - [12] S. S. Seahra, Phys. Rev. D **68**, 104027 (2003).
 - [13] R. Koley and S. Kar, Class. Quant. Grav. **22**, 753 (2005) and references therein.
 - [14] P. Kanti, K. A. Olive and M. Pospelov, Phys. Lett. B **481**, 386 (2000).
 - [15] S. Ghosh and S. Kar, Phys. Rev. D **80**, 064024, (2009).

- [16] S. H. Strogatz, *Nonlinear Dynamics and Chaos*, (Addison–Wesley Publishing Company, USA, 1994).